A Synthetic Route to Alkyl−Pt^{III} Dinuclear Complexes from Olefins and Its Implication on the Olefin Oxidation Catalyzed by Amidate-Bridged Pt^{III} Dinuclear Complexes

Kazuko Matsumoto,* Yuji Nagai, Jun Matsunami, Kazuhiro Mizuno, Takeya Abe, Ryosuke Somazawa, Jun Kinoshita, and Hideo Shimura

Contribution from the Department of Chemistry, Advanced Research Center for Science and Engineering, Waseda University, Shinjuku-ku, Tokyo 169, Japan

Received April 9, 1997

Abstract: Amidate-bridged Pt^{III} dinuclear complexes $[Pt_2(NH_3)_4(Am)_2(H_2O)_2]^{4+}$ (Am = amidate ligand) catalyze oxidation of olefins in acidic aqueous solution. Linear olefins are oxidized to ketones, whereas cyclic olefins are oxidized to epoxides. GC−MS analysis of the oxidation products obtained from the reaction in $H_2{}^{18}O$ showed that the oxygen atoms in the products are exclusively from water, suggesting that the reaction mechanism is basically similar to that of the Wacker reaction. In accordance with this mechanism, pivalamidate-bridged Pt^{III} complex $[Pt^{III}_2(NH_3)_4((CH_3)_3CCONH)_2(H_2O)_2]^{4+}$ has been found to react with olefins to give alkyl complexes. Reactions with 4-penten-1-ol and ethylene glycol vinyl ether in acidic aqueous solution gave $[Pt^{III}_2(NH_3)_4((CH_3)_3CCONH)_2(CH_2\overline{CH(CH_2)_3O})](NO_3)_3{\cdot}H_2O$ (**7**) and $[Pt^{III}_2(NH_3)_4((CH_3)_3CCONH)_2(CH_2CHO)](NO_3)_3{\cdot}H_2O$ (**9**), respectively. The two compounds have been structurally confirmed by X-ray diffraction analysis and ^1H, ^{13}C, and ^{195}Pt NMR spectroscopy. The ^1H NMR of **9** shows that both π- and σ-complexes exist in equilibrium in D_2O, although the X-ray structure is close to the σ-complex. High electrophilicity of the α-carbon atoms of the compounds has been shown in the reactions with OH^-. The above reactions with olefins can be a general route to prepare dimeric Pt^{III}−alkyl complexes.

Introduction

Amidate-bridged Pt^{III} dinuclear complexes $[Pt_2(NH_3)_4(Am)_2L_2]^{n+}$ (Am is amidate ligand and L is axial ligand, such as NO_3^-, NO_2^-, H_2O, and Cl^-) have been known for many years,[1−9] but their organometallic compounds having alkyl groups at the axial position remain to be explored. Due to the strong trans influence implemented by the alkyl ligand via the Pt−Pt bond to the other terminal axial ligand and the electron delocalization along the Pt−Pt bond, the axial ligands of such complexes are expected to exhibit novel reactivities that cannot be obtained with other Pt oxidation states.

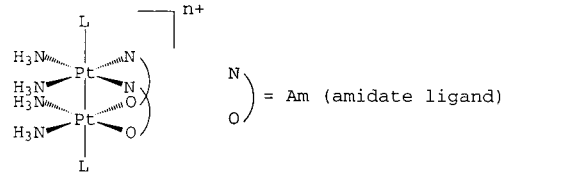

For instance, we have reported that acetonyl complex $[Pt^{III}_2(NH_3)_4((CH_3)_3CCONH)_2(CH_2COCH_3)(NO_3)]^{2+}$ is produced on addition of acetone to a Pt^{III} dimer complex with axial H_2O, $[Pt_2(NH_3)_4((CH_3)_3CCONH)_2(H_2O)_2]^{4+}$, in strongly acidic aqueous solution.[10] The mechanism of the Pt^{III}−C bond formation was thought to be either one of the following two reactions.

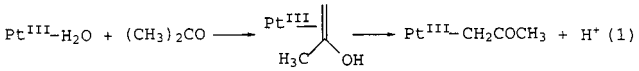

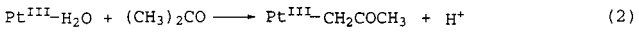

In eq 1, olefin coordination at the pt^{III}−Pt^{III} axial position is postulated as the initial step. Although olefin π-complex has not been isolated for any Pt^{III} complex, such π-complexes have been proposed as the intermediates of olefin ketonation and epoxidation reactions (Figure 1) catalyzed by amidate-bridged tetranuclear platinum blue complexes or Pt^{III} dinuclear complexes.[11] In these reactions cyclic olefins are selectively oxidized to epoxides, whereas linear olefins are oxidized to ketones and aldehydes.

In the oxidation reactions, water oxygen is incorporated into all of the products, which suggests that the reaction follows basically the mechanism of the Wacker reaction, and the product selectivity can be explained as follows. Sterically more restrained cyclic olefins do not undergo a 1,2-shift, thus giving epoxides, whereas sterically more flexible linear olefins give ketones after a 1,2-shift.[11] In the present study, an attempt was made to isolate the olefin π-complex of the Pt^{III} dimer in order

(1) Hollis, L. S.; Lippard, S. J. *Inorg. Chem.* **1983**, *22*, 2605.
(2) O'Halloran, T. V.; Roberts, M. M.; Lippard, S. J. *Inorg. Chem.* **1986**, *25*, 957.
(3) Lippert, B.; Schöllhorn, H.; Thewalt, U. *J. Am. Chem. Soc.* **1986**, *108*, 525.
(4) Hollis, L. S.; Lippard, S. J. *J. Am. Chem. Soc.* **1981**, *103*, 6761.
(5) Hollis, L. S.; Roberts, M. M.; Lippard, S. J. *Inorg. Chem.* **1983**, *22*, 3637.
(6) Hollis, L. S.; Lippard, S. J. *J. Am. Chem. Soc.* **1981**, *103*, 6761.
(7) Hollis, L. S.; Lippard, S. J. *Inorg. Chem.* **1982**, *21*, 2116.
(8) Abe, T.; Moriyama, H.; Matsumoto, K. *Chem. Lett.* **1989**, 1857.
(9) Abe, T.; Moriyama, H.; Matsumoto, K. *Inorg. Chem.* **1991**, *30*, 4198.
(10) Matsumoto, K.; Matsunami, J.; Mizuno, K.; Uemura, H. *J. Am. Chem. Soc.* **1996**, *118*, 8959.
(11) Matsumoto, K.; Mizuno, K.; Abe, T.; Kinoshita, J.; Shimura, H. *Chem. Lett.* **1994**, 1325.

S0002-7863(97)01129-3 CCC: $15.00
Published on Web 03/18/1998

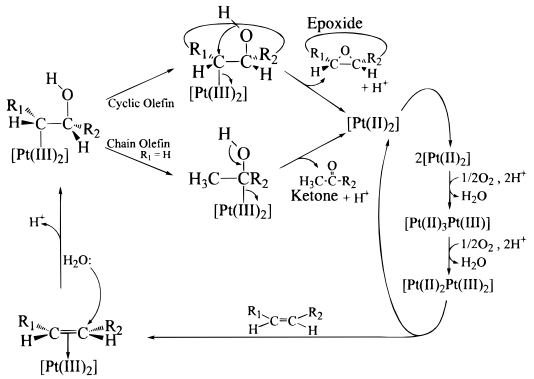

Figure 1. Proposed reaction mechanism for olefin ketonation and epoxidation catalyzed by platinum blue.

to prove the proposed mechanisms in eq 1 and Figure 1. While no olefin π-complex was obtained despite our intensive effort, 4-penten-1-ol and ethylene glycol vinyl ether were found to give alkyl complexes. This fact strongly supports the mechanisms in eq 1 and Figure 1. Although Figure 1 shows that tetranuclear platinum blue complexes catalyze the reactions, the actual species responsible for the reaction are Pt^{III} dinuclear complexes produced by disproportionation of the tetranuclear complexes, since the Pt^{III} dinuclear complexes also catalyze the olefin oxidation as efficiently as the tetranuclear platinum blue complexes.[11] The alkyl complexes formed in the present study are the 2-methyltetrahydrofurfuryl−Pt^{III} complex $[Pt_2(NH_3)_4((CH_3)_3CCONH)_2(CH_2\overline{CH(CH_2)_3O})](NO_3)_3\cdot H_2O$ and oxyethyl complex $[Pt_2(NH_3)_4((CH_3)_3CCONH)_2(CH_2CHO)](NO_3)_3\cdot H_2O$, which were obtained from the reaction of $[Pt_2(NH_3)_4((CH_3)_3CCONH)_2(H_2O)_2]^{4+}$ with 4-penten-1-ol and ethylene glycol vinyl ether, respectively. The reactions reported in the present paper support π-coordination of the olefins to the Pt^{III} axial position in the first step of the reaction, although π-coordination is very unstable and the π-complex cannot be isolated. The present reactions are also very important in that they give a general route for synthesizing alkyl−Pt^{III} dinuclear complexes.

Experimental Section

Preparation of the Platinum Blue Complexes and Pt^{III} Dinuclear Complexes Used as Catalysts. The platinum blue compound used as the catalyst $[Pt_4(NH_3)_8(C_4H_6NO)_4](NO_3)_6\cdot 2H_2O$ (**1**),[12,13] where C_4H_6NO is α-pyrrolidonate, was prepared according to the published method. Compound $[Pt_4(NH_3)_8(C_5H_{10}NO)_4](NO_3)_5$ (**2**), where $C_5H_{10}NO$ is pivalamidate, was prepared as follows. To a solution of *cis*-$[Pt(NH_3)_2(OH_2)_2](NO_3)_2$ (1 mmol in 5 mL of H_2O)[14] was added 1 mmol of pivalamide. After the solution was heated at 70 °C for 1 h, the color of the solution turned to blue-green. To the solution was added 0.3 g of $NaNO_3$, and the solution was left at 5 °C for 2−3 days. Dark green plate crystals of **2** were obtained with a yield of 18%. Single-crystal X-ray analysis confirmed that the complex cation has the usual tetranuclear platinum blue chain structure, which has been reported previously for other platinum blues.[12,13,15,16] Anal. Calcd for $Pt_4C_{20}H_{64}N_{17}O_{19}$: C, 14.76; H, 3.96; N, 14.63. Found: C, 14.55; H, 3.95; N, 14.29.

$[Pt_4(NH_3)_8(\alpha\text{-pyrrolidonato})_4](n\text{-}C_{12}H_{25}SO_3)_6$ (**3**) was prepared by adding excess $C_{12}H_{25}SO_3Na$ to the aqueous solution of **1** for precipitation. The precipitate was recrystallized from CH_2Cl_2. $[Pt_4(NH_3)_8(pivalamidato)_4](n\text{-}C_{12}H_{25}SO_3)_5$ (**4**) was prepared by addition of a 5-fold equivalent amount of n-$C_{12}H_{25}SO_3Na$ instead of $NaNO_3$ to the reaction solution of **2**. The pentahydrated form of **4** was obtained. The unhydrated form of **4** was obtained by recrystallization from CH_2Cl_2.

3-Methyl-2-pyrrolidonate-Bridged Platinum Tan Compound $[Pt_4(NH_3)_8(C_5H_8NO)_4](NO_3)_6\cdot 3H_2O$ (**5**) was synthesized similarly to **1**,[12,13] by using 3-methyl-2-pyrrolidone instead of α-pyrrolidone. Yield: 21%. Anal. Calcd for $Pt_4C_{20}H_{62}N_{18}O_{25}$: C, 13.80; H, 3.60, N, 14.50. Found: C, 13.60; H, 3.36; N, 14.40. 5-Methyl-2-pyrrolidonate-Bridged Platinum Blue Compound $[Pt_4(NH_3)_8(C_5H_8NO)_4](ClO_4)_5$ (**6**) was also prepared similarly to **1**,[12,13] by using 5-methyl-2-pyrrolidone and $NaClO_4$ instead of α-pyrrolidone and $NaNO_3$, respectively. Yield: 20%. Anal. Calcd for $Pt_4Cl_5C_{20}H_{56}N_{12}O_{24}$: C, 13.20; H, 3.12; N, 9.30. Found: C, 13.40; H, 3.12; N, 9.06.

Catalytic Olefin Oxidation. Since most of the platinum complexes are insoluble in dichloroethane, the reaction was carried out in a $H_2O-CH_2ClCH_2Cl$ biphasic solution. In a typical experiment, 10 μmol of the platinum complex and a 5-fold (**2, 4, 6**) or 6-fold (**1, 3, 5**) equivalent amount of phase transfer agent, $C_{12}H_{25}SO_3Na$, were dissolved in a mixture of 1 mL of 0.05 M H_2SO_4 and 1 mL of CH_2ClCH_2Cl containing a 400-fold equivalent amount of olefin. The solution was stirred vigorously in a closed O_2-filled Teflon vial (5 mL), which is placed in an O_2-filled glass bottle with a screw stopper to avoid O_2 leak from the Teflon vial. The reaction was carried out at 50 °C for 5 days, and an aliquot of the solution was analyzed with gas chromatography. The products were analyzed on a Shimadzu GC 4A gas chromatograph with anisol as the inner standard.

Preparation of $[Pt^{III}_2(NH_3)_4((CH_3)_3CCONH)_2(CH_2\overline{CH(CH_2)_3O}](NO_3)_3\cdot H_2O$ (7). Platinum pivalamidate blue, $[Pt_4(NH_3)_8((CH_3)_3CCONH)_4](NO_3)_5$ (**2**) (10 mg), in 0.01 M $HClO_4$ (0.8 mL) was oxidized to $[Pt_2(NH_3)_4((CH_3)_3CCONH)_2(H_2O)_2]^{4+}$ (**8**) with $Na_2S_2O_8$ (2.5 mg) by warming at 50 °C for 5 min. To the solution were added 4-penten-1-ol (10 μL) and concentrated HNO_3 (0.1 mL), and the solution was stirred for 1 day at room temperature. Pale yellow plate crystals of **7** were obtained with a yield of 63%. Anal. Calcd: C, 19.01; H, 4.57; N, 13.30. Found: C, 19.22; H, 4.36; N, 12.97.

Preparation of $[Pt^{III}_2(NH_3)_4((CH_3)_3CCONH)_2(CH_2CHO)](NO_3)_3\cdot H_2O$ (9). Compound **9** was prepared similarly to **7** by using 10 μL of ethylene glycol vinyl ether. Yellow plate crystals were obtained with a yield of 49%. Anal. Calcd: C, 15.94; H, 4.12; N, 13.93. Found: C, 15.92; H, 3.90; N, 13.78.

Preparation of the 4-*tert*-Butylbenzenesulfonate Salt of 8. This salt was prepared by dissolving 20 mg of **9** in 1 mL of water containing sodium 4-*tert*-butylbenzenesulfonate. The yellow-white precipitate obtained was dried over P_2O_5 under a light shield for a week. The compound was confirmed by ^{1}H NMR.

Reaction of 2 with Acetaldehyde. Compound **1** (10 mg) was oxidized with $Na_2S_2O_8$ in 1 mL of 0.01 M $DClO_4$ similarly to the preparation of **8**, to which 10 μL of 1 M CH_3CHO (1 equiv) in 0.01 M $DClO_4$ was added, and the solution was reacted at room temperature for 5 days. A similar reaction was carried out also in neutral water. The amount of acetaldehyde was also varied to 10 equiv. In all of the cases, CH_3CHO was exclusively oxidized to acetic acid and **8** was reduced to the corresponding Pt^{II} dimer complex.

Collection and Reduction of X-ray Data. Pale yellow plate crystals of **7** (0.50 mm × 0.30 mm × 0.05 mm) and yellow plate crystals of **9** (0.70 mm × 0.20 mm × 0.05 mm) were coated with epoxy resin for use in the X-ray diffraction study. Intensity data were collected on a Rigaku AFC-7R diffractometer using graphite-monochromated Mo Kα radiation (λ = 0.710 69 Å) at 27 °C. Three standard reflections were measured after 150 reflections. No decay correction was applied, since significant crystal deterioration was not observed. Empirical absorption correction based on azimuthal scans of several reflections was applied which resulted in transmission factors ranging from 0.32 to 1.00 (**7**) and from 0.29 to 1.00 (**9**). The data were corrected for Lorentz and polarization effects. Correction for secondary extinction was applied. Further details of the data collection procedures are summarized in Tables 1 and S1 and S2 in the Supporting Information.

Structure Solution and Refinement. A crystal analysis package, teXsan, was used. The structures were solved by the heavy-atom

(12) Matsumoto, K.; Fuwa, K. *J. Am. Chem. Soc.* **1982**, *104*, 897.
(13) Matsumoto, K.; Takahashi, H.; Fuwa, K. *Inorg. Chem.* **1983**, *22*, 4086.
(14) Sakai, K.; Matsumoto, K. *J. Mol. Catal.* **1990**, *60*, 1.
(15) Barton, J. K.; Best, S. A.; Lippard, S. J. *J. Am. Chem. Soc.* **1978**, *100*, 3785.
(16) Barton, J. K.; Caravana, C.; Lippard, S. J. *J. Am. Chem. Soc.* **1979**, *101*, 7269.

Table 1. Crystallographic Data

	7	**9**
chem formula	$Pt_2O_{13}N_9C_{15}H_{43}$	$Pt_2O_{13}N_9C_{12}H_{37}$
fw	947.74	905.66
cryst syst	triclinic	triclinic
space group	$P\bar{1}$ (no. 2)	$P\bar{1}$ (no. 2)
cryst params		
a (Å)	10.210(3)	10.166(3)
b (Å)	15.331(3)	14.616(4)
c (Å)	9.646(1)	9.541(2)
α (deg)	94.27(1)	96.77(2)
β (deg)	84.15(2)	93.95(2)
γ (deg)	89.66(2)	88.65(2)
V (Å^3)	1497.8(9)	1404.4(6)
Z	2	2
T (°C)	27	27
λ (Å)	0.71069	0.71069
ρ_{calcd} (g cm^{-3})	2.101	2.142
μ (cm^{-1})	93.63	99.80
transm factors	0.2935−1.0000	0.3166−1.0000
R	0.042	0.042
Rw ($w = 1/\sigma^2(F)$)	0.036	0.033

method. Successive Fourier synthesis revealed all the atoms. The non-hydrogen atoms were refined anisotropically, whereas the hydrogen atoms were included in the calculation but were not refined. The final cycle of the full-matrix (least-squares refinement based on 4679 observed reflections ($F > 3.00\sigma(F)$) and 353 parameters converged the *R* and *Rw* values to 0.042 and 0.036 for **7**. Those for **9** with 4801 observed reflections ($F > 3.00\sigma(F)$) and 326 parameters were 0.042 and 0.033. The definitions for *R* and *Rw* are $R = \sum||F_o| - |F_c||/\sum|F_o|$ and $Rw = [\sum w(|F_o| - |F_c|)^2/\sum w|F_o|^2]^{1/2}$, ($w = 1/\sigma^2(F_o)$). The largest peaks in the final difference Fourier syntheses were 0.95 e/Å^3 for **7** and 0.67 e/Å^3 for **9**. The final atomic positional and thermal parameters and the full interatomic distances and angles for **7** and **9** are given in Tables S1 and S2.

Results

Synthesis and Crystal Structures of 7 and 9. The crystal structures of **7** and **9** are shown in Figures 2 and 3, respectively. The reactions of 4-penten-1-ol and ethylene glycol vinyl ether with the amidate-bridged Pt^{III} dinuclear complex are expressed as eqs 3 and 4, respectively. Both **7** and **9** are not very stable in air and must be kept in a desiccator.

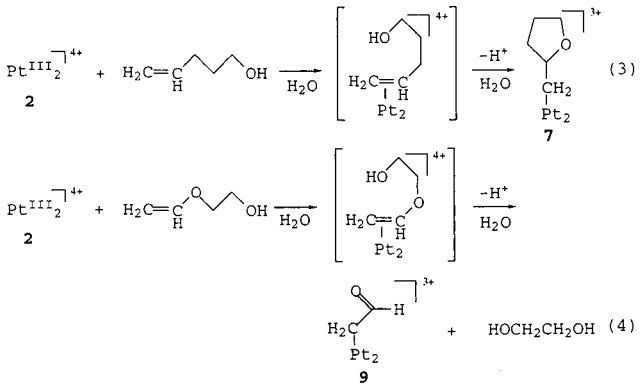

Selected bond distances (Å) and angles for **7** and **9** are listed in Tables 2 and 3. Both of the Pt−Pt distances (2.7687(8) Å in **7** and 2.7106(7) Å in **9**) are significantly longer than those in the previously reported amidate-bridged dinuclear Pt^{III} complexes with non-alkyl axial ligands such as halide, H_2O, NO_2^-, or NO_3^- (2.165(10)−2.644(1) Å).[1−9] The present long Pt−Pt distances are brought about by the strong trans influence of the alkyl ligand, and this strong trans influence extends further to the other axial end. Therefore, the Pt−O (axial nitrate)

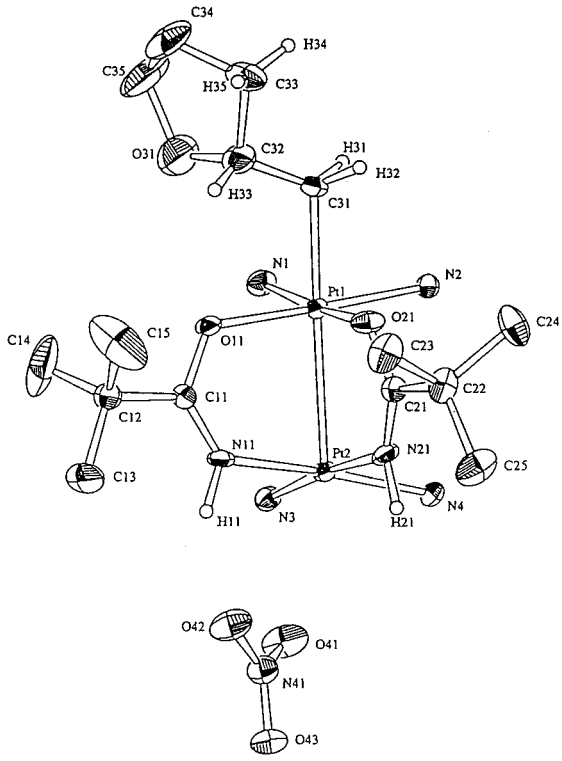

Figure 2. ORTEP drawing of $[Pt^{III}_2(NH_3)_4((CH_3)_3CCONH)_2(CH_2\overline{CH-(CH_2)_3O})](NO_3)_3\cdot H_2O$ (**7**).

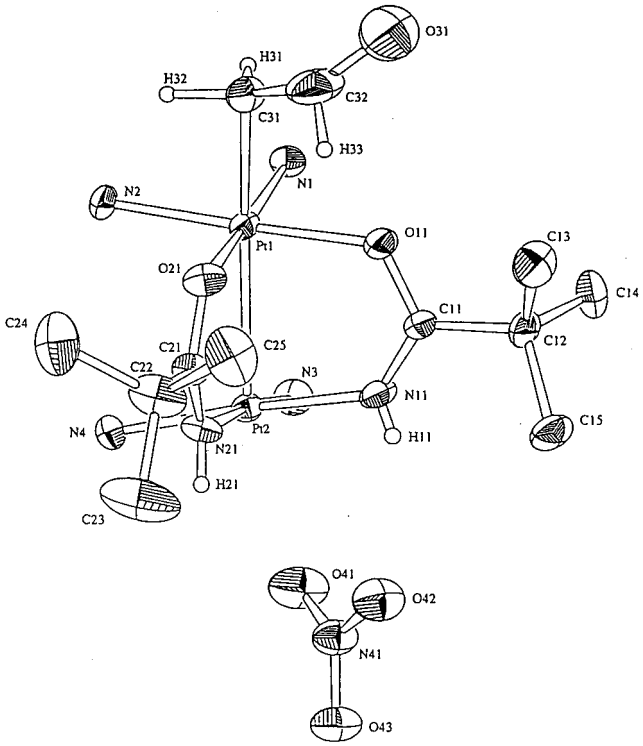

Figure 3. ORTEP drawing of $[Pt^{III}_2(NH_3)_4((CH_3)_3CCONH)_2(CH_2CHO)](NO_3)_3\cdot H_2O$ (**9**).

distances of **7** (2.92(1) Å) and **9** (2.7498(8) Å) are significantly longer than the usual nitrate coordination distances to Pt^{III} (2.71(1)−2.36(3) Å).[1−7] The Pt−O(axial nitrate) is so long that it is not a coordination bond anymore. Such a remote trans influence via a Pt−Pt bond would be caused by a strong dipole-inducing effect of the alkyl ligand, and a dipole structure along the Pt−Pt axis, R−Pt$^{\delta+}$−Pt$^{\delta-}$−L, is induced. Judging from

Table 2. Selected Bond Distances (Å) for **7** and **9**

compd	atom 1	atom 2	distance
7	Pt1	Pt2	2.7487(8)
	Pt1	C31	2.11(1)
	Pt1	O11	2.014(7)
	Pt1	O21	2.003(8)
	Pt1	N1	2.048(9)
	Pt1	N2	2.050(8)
	Pt2	N3	2.082(8)
	Pt2	N4	2.078(8)
	Pt2	N11	2.006(9)
	Pt2	N21	2.008(9)
	C31	C32	1.47(2)
	C32	C33	1.48(2)
	C33	C34	1.47(2)
	C34	C35	1.47(3)
	O31	C35	1.45(2)
	O31	C32	1.47(2)
9	Pt1	Pt2	2.7106(7)
	Pt1	C31	2.121(9)
	Pt1	O11	2.018(6)
	Pt1	O21	2.009(5)
	Pt1	N1	2.052(6)
	Pt1	N2	2.065(6)
	Pt2	N3	2.086(6)
	Pt2	N4	2.088(7)
	Pt2	N11	1.994(7)
	Pt2	N21	1.993(6)
	C31	C32	1.35(2)
	C32	O31	1.30(2)

Table 3. Selected Bond Angles (deg) for **7** and **9**

compd	atom 1	atom 2	atom 3	angle
7	Pt2	Pt1	O11	85.8(2)
	Pt2	Pt1	O21	85.5(2)
	Pt2	Pt1	N1	100.0(2)
	Pt2	Pt1	N2	96.1(2)
	Pt2	Pt1	C31	169.3(4)
	O11	Pt1	C31	91.1(4)
	O21	Pt1	C31	84.3(4)
	N1	Pt1	C31	90.1(5)
	N2	Pt1	C31	86.9(4)
	Pt1	Pt2	N3	104.5(2)
	Pt1	Pt2	N4	105.9(2)
	Pt1	Pt2	N11	79.6(2)
	Pt1	Pt2	N21	80.3(2)
9	Pt2	Pt1	O11	86.6(2)
	Pt2	Pt1	O21	85.7(2)
	Pt2	Pt1	N1	98.2(2)
	Pt2	Pt1	N2	95.9(2)
	Pt2	Pt1	C31	170.0(2)
	N1	Pt1	C31	90.9(3)
	N2	Pt1	C31	87.9(3)
	O11	Pt1	C31	89.3(3)
	O21	Pt1	C31	85.2(3)
	Pt1	Pt2	N3	104.1(2)
	Pt1	Pt2	N4	104.5(2)
	Pt1	Pt2	N11	79.5(2)
	Pt1	Pt2	N21	80.6(2)

the fact that one terminal of the Pt−Pt axis is bonded to an alkyl, while the other end does not have any axial ligand, the Pt atom bonded to alkyl (R) is close to Pt^{IV}, whereas the other Pt atom is close to Pt^{II}. This valence localization is also observed in the ^{195}Pt NMR spectra as detailed in a later section. Although the non-alkylated Pt^{III} dimer complex **8** might be considered as a mixed valent of Pt^{II} and Pt^{IV}, it does not show any band that can be ascribed to an IT (intervalence charge transfer) band in the range of 200−2000 nm. This suggests that the complex is a perfect Pt^{III} dimer. The alkylated Pt^{III} dimer complexes **7** and **9** also do not show such bands. The CT band in the UV region shifts to higher energies on alkylation.

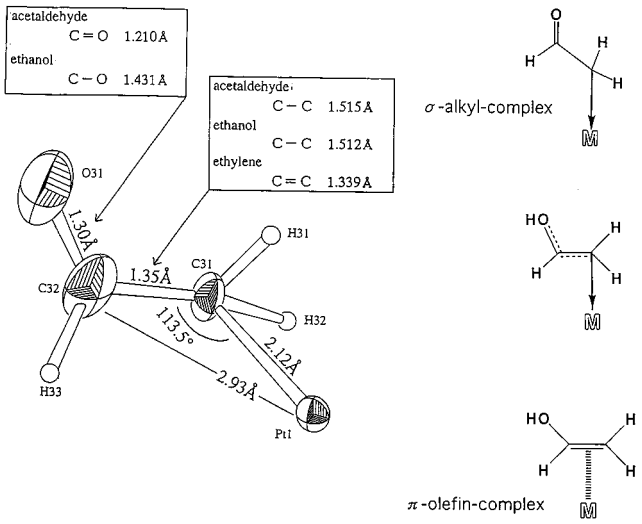

Figure 4. Bond distances and angles of the β-oxyethyl group in **9**.

The λ_{max} (nm)/$\epsilon_{\lambda_{max}}$ (M^{-1} cm^{-1}) in 0.01 M $HClO_4$ is (for **8**) 349/2.6 × 10^3 and 276/9.5 × 10^3 and (For **7**) 2.99/8.1 × 10^3 and 263/1.2 × 10^4.

The bond distances of the alkyl group in **9** are shown in Figure 4, together with the related C═C, C−C, C−O, and C═O distances. The C−C distance in **9** is intermediate between typical C−C and C═C distances, and the C−O distance of **9** is also between the typical C−O and C═O distances. This fact means that the actual electronic state of the alkyl group is an intermediate of the σ- and π-complexes as shown in Figure 4. The Pt−C−C angle of 113.5° in **9** is close to that of the σ-complex.

Discussion

Synthesis of 7 and 9. Both reactions 3 and 4 clearly demonstrate that (i) olefins coordinate to the Pt^{III} dimer and (ii) the coordinated olefins receive nucleophilic attack and produce alkyl complexes. These reactions are typical features of the Wacker reaction, and support the reaction mechanisms in Figure 1 as described later. Reactions 1, 3, and 4 also illustrate a general synthetic route for preparing alkyl−Pt^{III} dimer complexes. Although a number of olefin π-complexes are known for Pt^{II}, the coordinated olefins do not easily undergo nucleophilic attack unless it is in cationic complexes.[17−20] Only a few nucleophilic attacks are reported for neutral Pt^{II} complexes,[20b] and therefore it would be interesting to see whether neutral Pt^{III} complex, if it exists at all, undergoes a similar nucleophilic attack. On the other hand, olefin does not coordinate to Pt^{IV}, and therefore no π-complex and alkyl complex derived therefrom are known with Pt^{IV}. In this regard, the present reactions prove for the first time that Pt^{III} complexes can coordinate olefins, undergo nucleophilic attack, and be easily converted to more stable alkyl complexes. This higher stability of the Pt^{III}−alkyl complexes over the corresponding Pt^{III} π-complexes would be due to the high oxidation state of Pt^{III}, which is less π-back-donating and more electron-withdrawing than Pt^{II}. The strong electron withdrawal of Pt^{III} would raise

(17) Eisenstein, O.; Hoffman, R. *J. Am. Chem. Soc.* **1981**, *103*, 4308.
(18) Fanizzi, F. P.; Intini, F. P.; Maresca, L.; Natile, G.; Gasparrini, F. *J. Chem. Soc., Dalton Trans.* **1990**, 1019.
(19) Fanizzi, F. P.; Intini, F. P.; Maresca, L.; Natile, G. *J. Chem. Soc., Dalton Trans.* **1992**, 309.
(20) (a) Maresca, L.; Natile, G. *J. Am. Chem. Soc.* **1982**, *104*, 7661. (b) Panunzi, A.; De Renzi, A.; Palumbo, R.; Paiaro, G. *J. Am. Chem. Soc.* **1969**, *91*, 3879.

the $\delta+$ nature of the coordinated olefin, which then easily receives nucleophilic attack by the hydroxy group as shown in eqs 3 and 4. The unexpectedly high stability of the $Pt^{III}-$alkyl complexes in acidic aqueous solution should be noted; this would be a result of the strong electron withdrawal of the Pt^{III} atom from the alkyl.

Complex **9** could not be directly prepared from acetaldehyde and **8**, analogously to the preparation of **9**.[10] Instead, acetaldehyde is oxidized to acetic acid by **8** and **8** is reduced to the corresponding Pt^{II} dimer complex. No intermediate was observed with ^{1}H NMR spectroscopy. Since dissolution of **9** in neutral water or 0.1 M $DClO_4$ produces glycol aldehyde as well as acetic acid, it seems that **9** is not formed in the reaction of **8** with acetaldehyde.

Chemical Reactivities. Although complexes **7** and **9** do not prove directly the existence of olefin π-complexes, the present reactions strongly support the mechanism in Figure 1, indicating that an alkyl complex is produced by nucleophilic attack of H_2O on the olefinic carbon of the π-complex.

Complex **7** is stable in acidic to weakly basic aqueous solution. However, on addition of 0.1 M NaOH, nucleophilic attack at the β-carbon takes place as shown in eq 5. In this reaction, it may also be considered that α-hydroxylation takes place initially, which eventually leads to dehydration to give the product.

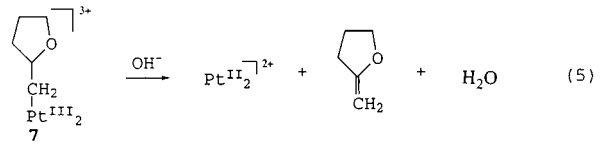

(5)

7

Complex **9** is unstable at room temperature even as a solid and is easily hydrolyzed in neutral water to produce glycol aldehyde (eq 6). In 0.1 M $HClO_4$, **9** produces glycol aldehyde and acetic acid in a ca. 9:1 ratio.

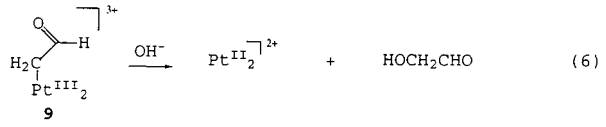

(6)

9

The absence of the attack of the α-carbon by OH^- for **7** in contrast to the reaction in eq 6 would be due to the electron donation by the β-carbon in **7**. Addition of ethylene glycol vinyl ether to the *p*-toluenesulfonate salt of **8** in $CDCl_3$ catalytically yields 2-methyl-1,3-dioxolane (eq 7). The reaction proceeds

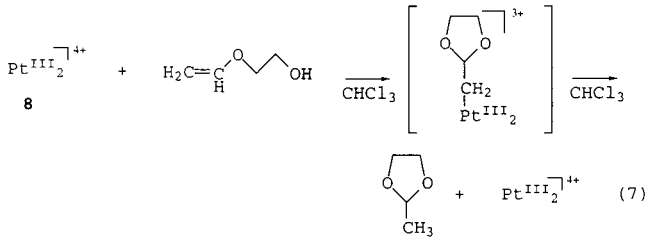

(7)

8

almost instantaneously, and a 50-fold equivalent of the substrate is completely converted to 2-methyl-l,3-dioxolane, which was confirmed by ^{1}H NMR. After the reaction, the Pt^{III} dimer complex without an alkyl ligand is left in the solution, which is still capable of the catalysis. The reaction can be drawn as in eq 7.

Similar reaction was not observed for 4-penten-1-ol. It should be noted that a Pt^{III} dimer complex is released after the reaction in eq 7, which is contrasted with the release of olefin and a

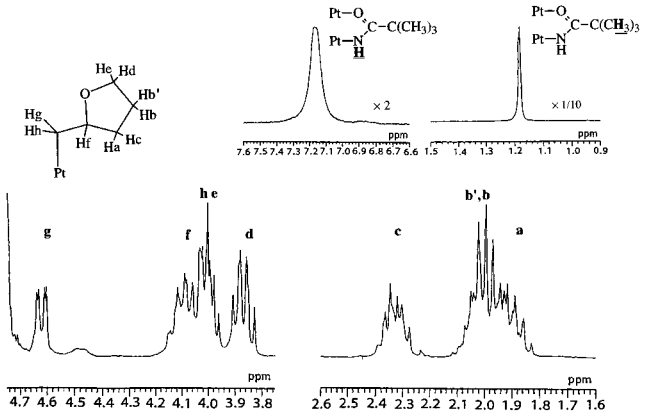

Figure 5. ^{1}H NMR spectrum of **7** in D_2O.

Pt(II) dimer complex in aqueous solution by reductive elimination (eq 5). The difference of such reactivity depending on the alkyl and the solvent would be caused by the difference of the electron density of the α-carbon atom and the dipole structure along the Pt−Pt bond in the solvents of different polarity. In aprotic organic solvent, the electron distribution along the Pt−Pt bond would be less polar, i.e., close to $R-Pt^{III}-Pt^{III}$, whereas in aqueous solution, it would be more polar, being close to $R-Pt^{IV}-Pt^{II}$, as indicated in the X-ray structure of **7**. Recent work of Labinger and Bercaw's group on the C−H activation of an alkane by a mixture of Pt^{II} and Pt^{IV} shows that $R-Pt^{IV}$ receives nucleophilic attack by Nu: to release NuR and Pt^{II}; no such behavior is observed for $R-Pt^{II}$.[21−23] It is therefore reasonable that $R-Pt^{IV}-Pt^{II}$ undergoes nucleophilic attack by OH^- to release ROH or olefin and a Pt^{II} dinuclear complex in aqueous solution. Although it is essential to compare the reactivity of an identical compound in organic and aqueous solutions, **7** and **9** cannot be dissolved in organic solvents, and exhibit complicated decomposition if dissolved forcedly with the aid of a surfactant.

IR and NMR Characterization of Compounds 7 and 9. Both **7** and **9** do not have an IR band around 1640 cm^{-1}, which is observed in the free olefins and ascribed to C═C. Compound **9** has its C═O band at 1688 cm^{-1}, which is shifted from 1726 cm^{-1} of the free acetaldehyde.

The ^{1}H, ^{13}C, and ^{195}Pt NMR spectra of **7** are shown in Figures 5−7. The assignment of the ^{1}H NMR spectrum was assisted by using the ^{1}H−^{1}H COSY spectrum (Figure S4). The ^{13}C chemical shifts (ppm) are as follows: C_a, 27.90; C_b, 29.23, 29.51; C_c, 30.97; C_d, 42.27, 42.37; C_e, 54.38; C_f, 71.13; C_g, 81.75; C_h, 195.01, 195.21. The chemical shift −272 ppm of Pt_b in Figure 7 is very low-field as a Pt^{III} complex, and indicates that the actual oxidation state of Pt_b would be close to Pt^{IV}. This fact corresponds well with the Pt oxidation states deduced from the X-ray structure, as discussed in an earlier section. The ^{1}H NMR spectrum of **9** in D_2O is shown in Figure 8. Different from what is expected for the crystal structure of **9**, two sets of signals (σ and π) are observed, whose relative intensities reversibly vary depending on the pH. These peaks are assigned as the acid−base equilibrium between π-vinyl alcohol and β-oxoethyl forms as shown in Figure 8. The ^{1}H chemical shifts of compound **9** are listed in Table 4. The assignment of the peaks has been confirmed by the ^{1}H−^{1}H COSY spectrum

(21) Stahl, S. S.; Labinger, J. A.; Bercaw, J. E. *J. Am. Chem. Soc.* **1996**, *118*, 5961.

(22) Labinger, J. A.; Herring, A. M.; Lyon, D. K.; Luinstra, G. A.; Bercaw, J. E. *Organometallics* **1993**, *12*, 895.

(23) Luinstra, G. A.; Wang, L.; Stahl, S. S.; Labinger, J. A.; Bercaw, J. E. *J. Organomet. Chem.* **1995**, *504*, 75.

Table 4. ^{1}H NMR Chemical Shifts and Coupling Constants for **9** in D_2O

	π-complex	σ-complex		π-complex	σ-complex
$\delta(H_a)$, ppm	1.18	1.17	$^3J(H_b-H_c)$, Hz	4.3	4.3
$\delta(H_b)$, ppm	4.19	4.88	$^2J(Pt-H_b)$, Hz	69	
$\delta(H_c)$, ppm	5.01	10.05			

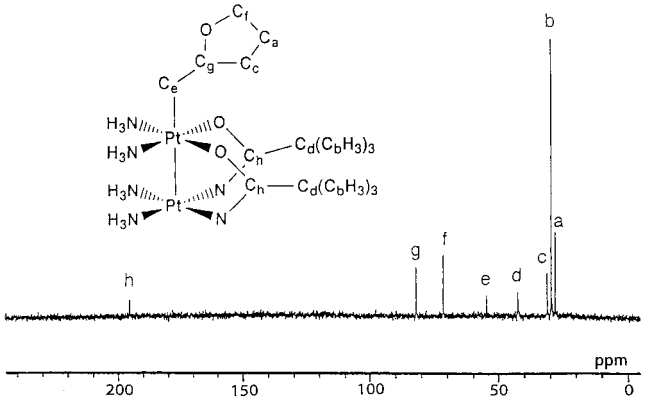

Figure 6. ^{13}C NMR spectrum of **7** in D_2O.

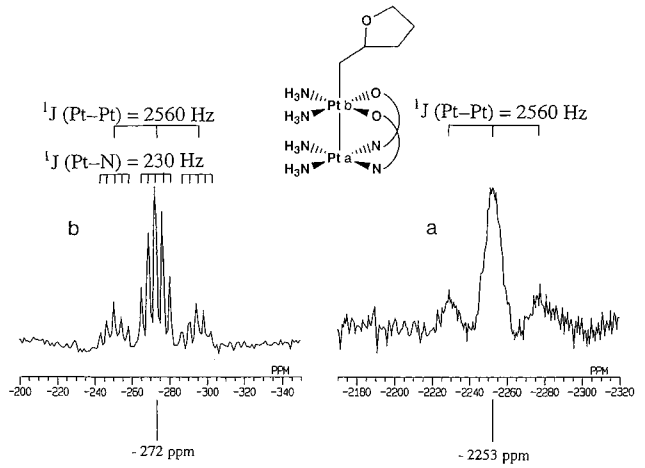

Figure 7. ^{195}Pt NMR spectrum of **7** in D_2O.

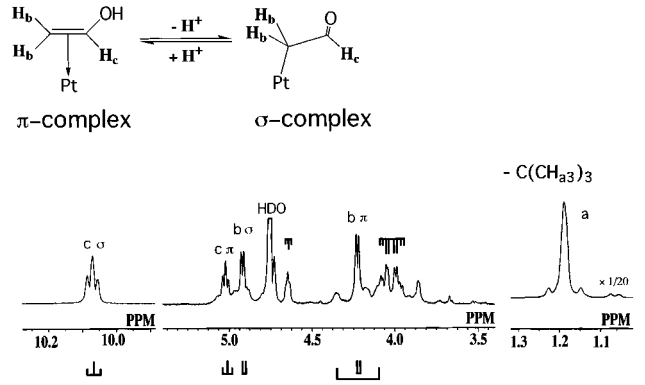

Figure 8. ^{1}H NMR spectrum of **9** in D_2O. The small peaks at around 4.0 and 4.6 ppm are not known. They are probably decomposition products.

(Figure S5). Similar acid−base equilibrium between π- and σ-complexes is reported for the vinyl alcohol−Pt^{II} complex in acetone,[24,25] in which, however, the two forms do not give

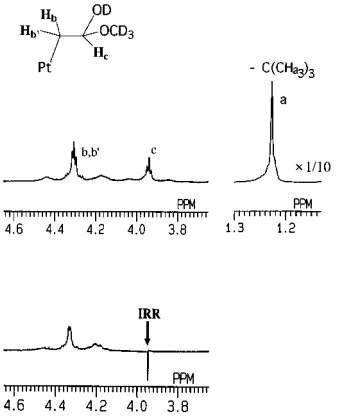

Figure 9. ^{1}H NMR spectrum of the 4-*tert*-butylbenzenesulfonate salt of **9** in CD_3OD. The originally triplet signal at 4.27−4.36 ppm becomes an AB-pattern signal on homonuclear decoupling at 3.94 ppm (the lower figure with IRR).

separate signals and appear at an intermediate chemical shift of those of the two forms. In both of the Pt^{II} and the present Pt^{III} compounds, the two H_b protons are equivalent, giving only a doublet for these protons and a triplet signal for the H_c proton. The spectral pattern of the π-complex of **9** is an A_2X pattern, although from the X-ray structure, it is expected to be ABX. A similar A_2X pattern is also observed in the vinyl alcohol π-complex of Pt^{II} in acetone.[24,26] The reason for the A_2X pattern in **9** is probably as follows. The π-complex of **9** is in equilibrium with a dihydroxyethyl form, and exchange of the two forms is rapid, as shown below.

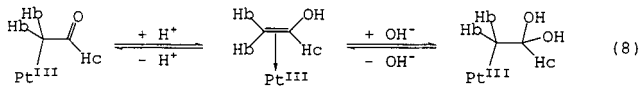

As an indirect support for this dihydroxyethyl complex, the ^{1}H NMR spectrum of the 4-*tert*-butylbenzenesulfonate salt of **9** was measured in CD_3OD (Figure 9), which shows a hemiacetal structure: H_a, 1.23, s, 18H; H_b, 4.31, dd, 1H; $H_{b'}$, 4.35, dd, 1H; H_c, 3.94, dd, 1H; $^2J(Pt-H_{b,b'}) \approx 75$ Hz; $^3J(Pt-H_c) = 54.0$ Hz. To confirm that OMe is attached to the ligand, the same compound was measured in THF-d_8-CH_3OH, 5:1 v/v, and a methoxy singlet signal was observed at 3.45 ppm with a 3H integral intensity.

The crystal structure of the vinyl alcohol−Pt^{II} complex is a π-complex with a lengthened C=C bond[25] with a pK_a of 3.5. Our compound **9** is close to a σ-complex in crystal structure although it is isolated from strongly acidic solution. This indicates that the conjugate acid form of **9** is a stronger acid than the vinyl alcohol−Pt^{II} complex, which would be due to the stronger electron-withdrawing effect of Pt^{III}, compared to Pt^{II}. Although it is important to measure the pK_a of **9**, it was not possible since the compound is too unstable in aqueous solution over the necessary pH range.

Catalytic Olefin Oxidation. The results of the olefin oxidation catalyzed by **1** to **6** are summarized in Tables 5−7.

(24) (a) Tsutsui, M.; Ori, M.; Francis, J. *J. Am. Chem. Soc.* **1972**, *94*, 1414. (b) Wakatsuki, Y.; Nozakura, S.; Murahashi, S. *Bull. Chem. Soc. Jpn.* **1969**, *42*, 273

(25) Cotton F. A.; Francis, J. N.; Frenz, B. A.; Tsutsui, M. *J. Am. Chem. Soc.* **1973**, *95*, 2483.

(26) Hillis, J.; Francis, J.; Ori, M.; Tsutsui, M. *J. Am. Chem. Soc.* **1974**, *96*, 4800.

Table 5. Olefin Oxidation Catalyzed by Platinum Blue Compounds

substrate	product	turnover number[a] catalyst **1**	catalyst **2**
1-hexene	2-hexanone	11.9	3.8
	1,2-epoxyhexane	8.6	8.8
1-heptene	2-heptanone[b]	13.3	4.5
1-octene	2-octanone[b]	15.8	12.4
1-decene	2-decanone	10.9	4.1
2-octene	2-octanone	1.7	1.6
	3-octanone	2.2	1.6
cyclohexene	epoxycyclohexane	22.8	15.0
	cyclohexanone[c]	1.9	1.4
cyclopentene	cyclopentanone	2.0	2.5
norbornene	epoxynorbornane	7.2	5.2
	norbornanone[d]	2.3	0.6
2-methyl-2-butene	3-methyl-2-butanone		
ethyl vinyl ether	acetaldehyde		
	ethyl alcohol		
1-chloro-1-propene		no reaction	
1-bromo-1-propene		no reaction	
α-methylstyrene		no reaction	
β-methylstyrene		no reaction	
allylbenzene		no reaction	

[a] Turnover number = [product]/[complex]. [b] Minor product (less than 1%) 1,2-epoxide. [c] Minor product (less than 1%) cyclopentanecarboxyaldehyde. [d] Minor product (less than 1%) norborneol.

Table 5 shows that linear terminal olefins are selectively oxidized to 2-ketones, whereas cyclic olefins (cyclohexene and norbornene) are selectively oxidized to epoxides. Cyclopentene shows exceptional behavior; it is oxidized exclusively to cyclopentanone without any production of epoxypentane. This exception would be brought about by the more-restrained and planar pentene ring, compared with other larger cyclic nonplanar olefins in Table 5, but the exact reason is not yet known. Linear inner olefin 2-octene is oxidized to both 2- and 3-octanones. 2-Methyl-2-butene is oxidized to 3-methyl-2-butanone, while ethyl vinyl ether is oxidized to acetaldehyde and ethyl alcohol. These products were identified by NMR, but could not be quantitatively determined because of the existence of overlapping small peaks in the GC chart. The last reaction corresponds to oxidative hydrolysis of ethyl vinyl ether. Those olefins having bulky (α-methylstyrene, *β*-methylstyrene, allylbenzene) or electron-withdrawing substituents (1-bromo-1-propene, 1-chloro-1-propene, fumalonitrile, acrylonitrile, and methylacrylate) are not oxidized.

Effect of the Experimental Conditions. Since it is known that the tetranuclear mixed-valent platinum blue complexes such as **1** and **2** undergo disproportionation and reduction by water as eqs 9−12 show,[27,28] all the species appearing in eqs 9−12

$$[Pt^{II}_2Pt^{III}_2(NH_3)_8(Am)_4]^{6+} \rightleftharpoons [Pt^{II}_2(NH_3)_4(Am)_2]^{2+} + [Pt^{III}_2(NH_3)_4(Am)_2(H_2O)_2]^{4+} \quad (9)$$

$$2[Pt^{II}_3Pt^{III}(NH_3)_8(Am)_4]^{5+} \rightleftharpoons 3[Pt^{II}_2(NH_3)_4(Am)_2]^{2+} + [Pt^{III}_2(NH_3)_4(Am)_2(H_2O)_2]^{4+} \quad (10)$$

$$2[Pt^{II}_2Pt^{III}_2(NH_3)_8(Am)_4]^{6+} + H_2O \rightleftharpoons 2[Pt^{II}_3Pt^{III}(NH_3)_8(Am)_4]^{5+} + 1/2\ O_2 + 2H^+ \quad (11)$$

$$[Pt^{II}_3Pt^{III}(NH_3)_8(Am)_4]^{5+} + 1/2\ H_2O \rightleftharpoons 2[Pt^{II}_2(NH_3)_4(Am)_2]^{2+} + 1/4\ O_2 + H^+ \quad (12)$$

are present in the solution. However, only one or several of the four species in the solution may in fact be active to the catalytic olefin oxidation. To clarify this point, the effect of the Pt oxidation state in the platinum complexes was compared. The results are summarized in Table 6, which clearly shows that the Pt^{III} dinuclear complex is most effective and would be the real catalyst. Compound **1** also exhibits high activity, whereas the Pt^{II} dinuclear complex is ineffective. All other factors expected to affect the catalysis efficiency including the presence of O_2 and surfactant and selection of solvent have been examined, and the results are summarized in Table 7. It is clear from runs 2, 3, and 4 that O_2 is indispensable to the oxidation reaction. Addition of surfactant or the presence of surfactant as the counterion is necessary (runs 2, 5, 10, 11, 13, and 14), and the reaction must be carried out in a biphasic solution, i.e., a mixture of CH_2ClCH_2Cl and 0.05 M H_2SO_4. Neither 0.05 M H_2SO_4 nor CH_2ClCH_2Cl alone gave appreciable products even with addition of surfactant (runs 6 and 7). It is also clear that water is essential to the reaction (runs 6 and 9). Acid is also necessary to the reaction; the oxidation does not proceed in a biphasic solution of H_2O/CH_2ClCH_2Cl (run 8). The effect of various acids was also examined, and the result showed that $HClO_4$ was as effective as H_2SO_4, while other coordinating acids, such as HNO_3 and HCl, were much less effective. The effect of a substituent on the α-pyrrolidone ring is compared in runs 2, 15, and 16, and it is evident that a substituent near the amidate group of the α-pyrrolidonate ring suppresses the reaction (run 16).

Table 6. Effect of the Platinum Oxidation State in the Catalytic Oxidation of Cyclohexene

catalyst	turnover number product epoxycyclohexane	product cyclohexanone
$[Pt^{III}_2(NH_3)_4(C_4H_6NO)_2(H_2O)_2](NO_3)_4$[a]	24.7	1.4
$[Pt^{II}_2Pt^{III}_2(NH_3)_8(C_4H_6NO)_4](NO_3)_6$ (**1**)	22.8	1.9
$[Pt^{II}_2(NH_3)_4(C_4H_6NO)_2](NO_3)_2$[b]	0.5	1.8

[a] The complex was prepared *in situ* by electrochemical oxidation at 0.60 V vs SCE.[8] [b] The complex was prepared *in situ* by electrochemical reduction at 0.35 V vs SCE.[8]

Although the olefins seem to be oxidized by O_2 from the experiments described above, GC−MS analysis of the oxidation products showed that all of the oxygen atoms in the products are from H_2O and not from O_2, as the following experiment shows. The oxidation reactions were carried out in both $^{16}O_2$ and $^{18}O_2$, and the products were analyzed with GC−MS. Contrary to our expectation, all of the oxygen atoms in the products including ketones and epoxides were ^{16}O, irrespective of whether the reaction had been carried out in $^{16}O_2$ or $^{18}O_2$. In the next step, the reactions were carried out in $^{16}O_2$ with either $H_2{}^{18}O$ or $H_2{}^{16}O$. The GC−MS analysis of the products (Figures S1 and S2) revealed that water oxygen is exclusively introduced into ketones and epoxides. The reactions were also carried out under $^{16}O_2$ in $D_2{}^{16}O$, and it was confirmed that deuterium does not exist in the products (Figure S3). From these facts, the mechanism of the catalytic oxidation of olefins to ketones and epoxides seems to be similar to the Wacker reaction,[29,30] as shown in Figure 1 for ketones and epoxides. There exist, however, several differences in the reactivities of the present reaction and the Wacker process: (i) epoxide is not produced as a main product in the Wacker process and (ii) inner olefins are not oxidized in the Wacker process, whereas they are

(27) Sakai, A.; Tsubomura, H.; Matsumoto, K. *Inorg. Chim. Acta* **1993**, *213*, 11.
(28) Matsunami, J.; Urata, T.; Matsumoto, K. *Inorg. Chem.* **1995**, *34*, 202.
(29) Bäckvall, J. E.; Åkermark, B.; Ljunggren, S. O. *J. Am. Chem. Soc.* **1979**, *101*, 2411.
(30) Stille, J. K.; Divakaruni, R. *J. Organomet. Chem.* **1979**, *169*, 239.

Table 7. Effects of Surfactant, Solvent, and Atomosphere on the Catalytic Oxidation of Cyclohexene

run	catalyst	surfactant[a] $C_{12}H_{25}SO_3Na$	solvent	atmosphere	turnover number: product epoxycyclohexane	turnover number: product cyclohexanone
1	none	+	0.05 M H_2SO_4/CH_2ClCH_2Cl	O_2	0	0.4
2	**1**	+	0.05 M H_2SO_4/CH_2ClCH_2Cl	O_2	22.8	1.9
3	**1**	+	0.05 M H_2SO_4/CH_2ClCH_2Cl	air	18.6	1.2
4	**1**	+	0.05 M H_2SO_4/CH_2ClCH_2Cl	N_2	4.7	0.8
5	**1**	−	0.05 M H_2SO_4/CH_2ClCH_2Cl	O_2	0	0.8
6	**1**	+	CH_2ClCH_2Cl	O_2	0	0
7	**1**	+	0.05 M H_2SO_4	O_2	0	0.3
8	**1**	+	H_2O/CH_2ClCH_2Cl	O_2	2.3	0.1
9	**1**	+	CF_3SO_3H[b]/CH_2ClCH_2Cl	O_2	0	0
10	**3**	+	0.05 M H_2SO_4/CH_2ClCH_2Cl	O_2	20.3	1.5
11	**3**	−	0.05 M H_2SO_4/CH_2ClCH_2Cl	O_2	17.3	1.2
12	**2**	+	0.05 M H_2SO_4/CH_2ClCH_2Cl	O_2	15.0	1.4
13	**4**	+	0.05 M H_2SO_4/CH_2ClCH_2Cl	O_2	14.5	1.0
14	**4**	−	0.05 M H_2SO_4/CH_2ClCH_2Cl	O_2	12.2	0.7
15	**5**	+	0.05 M H_2SO_4/CH_2ClCH_2Cl	O_2	21.7	1.3
16	**6**	+	0.05 M H_2SO_4/CH_2ClCH_2Cl	O_2	4.2	0.3

[a] +, added; −, not added. [b] Two drops of CF_3SO_3H added to CH_2ClCH_2Cl.

oxidized in the present reaction. For linear olefins, a 1,2-shift of the coordinated Pt takes place, giving selectively ketones or aldehydes, while for sterically more restrained cyclic olefins, a 1,2-shift does not take place and epoxides are formed as major products. Similar ketone vs epoxide selectivity based on the ease of the 1,2-shift has been proposed for olefin oxidation catalyzed by [Pt(diphoe)(CF_3)(OH)][31] (diphoe = *cis*-1,2-bis-(diphenylphosphino)ethene), where peroxide is used as the oxidizing agent.

During the reaction, most of the platinum complex is transferred to the organic phase as is observed with the dark blue or tan color of the tetranuclear complexes in the organic phase. After the catalytic reaction ceases, both phases are pale yellow. The tan color and the catalytic reaction can be recovered at this stage by adding sodium persulfate to the solution. This indicates that the Pt^{III} catalyst is gradually reduced to a Pt^{II} dinuclear complex, [Pt$^{II}_2$(NH_3)$_4$(Am)^2]$^{2+}$,[27,28] during the catalytic reaction, and the reaction finally stops. Acid and O_2 are necessary in the catalysis to reoxidize the Pt^{II} dinuclear complex to a Pt^{III} dinuclear complex.[28,32] The oxidation reaction is however not fast enough, and the reduced Pt^{II} dinuclear species gradually accumulates in the solution. Addition of $Na_2S_2O_8$ from the beginning of the reaction in order to increase the lifetime of the catalyst, however, decreases the turnover number.

Conclusion

Synthesis of **7** and **9** supports the olefin oxidation mechanism in Figure 1. This mechanism has several important and noteworthy points concerning Pt^{III} chemistry: (i) Olefins coordinate to Pt^{III} at the axial position, which is contrasted to the π-coordination of olefins perpendicular to the square planar coordination plane of Pt^{II}. Olefin coordination to Pt^{III} should also be contrasted with the fact that olefin does not coordinate to Pt^{IV}. (ii) Pt^{III} is strongly electron-withdrawing, and the coordinated olefins receive nucleophilic attack. (iii) The alkyl α-carbon on the Pt^{III} undergoes nucleophilic attack in aqueous solution, whereas in aprotic solvent, aldehyde (and possibly also ketone in other cases) is produced by reductive elimination.

The Pt^{III}−Pt^{III} bond in the alkyl complexes exhibits unique character that the Pt atom acts both as Pt^{II} and Pt^{IV} or the intermediate through electron delocalization along the Pt−Pt axis: (i) coordination of olefin is a Pt^{II} characteristic, since no olefin−Pt^{IV} complex is known and (ii) nucleophilic attack on the coordinated alkyl α-carbon atom takes place, which is a Pt^{IV} characteristic, and does not occur on α-carbon atoms of alkyl−Pt^{II} complexes.[22,23,33]

The electron localization (Pt^{IV}−Pt^{II}) and delocalization (Pt^{III}−Pt^{III}) through the Pt−Pt bond seem to depend on the nature of the axial alkyl ligand and polarity of the solvent. With this unique electron buffer function of the Pt−Pt bond, the present alkyl complexes are stabilized and exhibit various reactivities. The relative stability of the alkyl (σ) to olefin (π) complex on Pt^{III} and Pt^{II} can be easily seen by comparison of the crystal structures of the vinyl alcohol π-complex of Pt^{II} [24,25] and 2-oxyethyl σ-alkyl complex of Pt^{III} (compound **9**). The bond distances and angles in Figure 4 suggest that although **9** is a σ-complex, the ligand is actually the intermediate state between the σ-alkyl and π-olefin complexes. This should be compared to the structure of the π-complex of Pt^{II} with vinyl alcohol,[24,25] and suggests that since Pt^{III} is more strongly electron-withdrawing than Pt^{II}, the coordinated vinyl alcohol on Pt^{III} is more acidic, and thus the alkyl complex is more favored than that of Pt^{II}.

As for the reactivity of these alkyl−Pt^{III} complexes, it is notable that the σ-carbon can be either a nucleophile (eq 7) or an electrophile (eq 6) depending on the solvent and the alkyl group. What is more noteworthy is the reaction of eq 5. The σ-carbon of complex **7** does not receive nucleophilic attack by OH^-, presumably because the σ-carbon of **7** is more electron-rich than that of **9**.

Supporting Information Available: Full tables of the data collection parameters, isotropic and anisotropic temperature factors, and bond distances and angles for **7** and **9** and GC−MS and NMR data (43 pages). See any current masthead page for ordering information and Web access instructions.

JA971129K

(31) Strukul, G.; Sinigalia, R.; Zanardo, A.; Pinna F.; Michelin, R. A. *Inorg. Chem.* **1989**, *28*, 554.
(32) Sakai, K.; Tsubomura, T.; Matsumoto, K. *Inorg. Chim. Acta* **1995**, *234*, 157.
(33) Sen, A.; Lin M.; Kao, L. C.; Hutson. A. C. *J. Am. Chem. Soc.* **1992**, *114*, 6385.